Advances in Materials Research, *Vol. 14, No. 2 (2025) 173-184*
https://doi.org/10.12989/amr.2025.14.2.173

Comprehensive analysis of predictive efficiency of stress-strain models for concrete under uniaxial compression

Gopal Paliwal* and Shiwanand R. Suryawanshi[a]

Department of Civil Engineering, Sardar Vallabhbhai National Institute of Technology, Surat, Gujarat, India 395007

(*Received November 6, 2024, Revised April 4, 2025, Accepted April 21, 2025*)

Abstract. Most studies on stress-strain relationships in compression have relied on limited experimental data, resulting in models that often lack general applicability. This study aimed to evaluate the relevance and accuracy of existing stress-strain models across a range of concrete grades. Graphical, analytical and statistical methods were used to compare the predicted and measured stress-strain responses. Whereby ten stress-strain curves for normal to high strength concrete, with peak compressive stresses ranging between 18 MPa to 121 MPa, were selected and applied to selected established stress-strain models from the literature. The graphical comparison assessed ability of each model to replicate both the ascending and descending branches of the stress-strain curve in a normalized format. To further assess predictive performance analytically, each selected model was evaluated based on normalized toughness and ductility index. Additionally, root mean square error and coefficient of variation were calculated to statistically validate the accuracy of the predictions. The conclusion of this study indicate that most models were found to inadequately capture both the ascending and descending branches of the stress-strain curve across all concrete grades. While the best-performing model achieved higher accuracy, involved multiple equations, making it complex to implement. These findings highlight the need for a novel model that incorporates easily measurable parameters, such as compressive strength and uses a single equation to predict both branches of the curve, ensuring broad applicability across concrete grades.

Keywords: high strength concrete; load-deformation behaviour; normal strength concrete; stress-strain relationship

1. Introduction

The use of concrete in construction projects around the world is experiencing a steady and significant increase. This trend can be attributed to the unique and advantageous properties of concrete, which make it an indispensable material in civil engineering. Among its many benefits, concrete is known for its excellent compressive strength, durability, versatility and adaptability to various structural requirements. These properties allow it to be used across a wide range of applications, from residential buildings and commercial complexes to large-scale infrastructure projects such as bridges, highways and dams etc. As the field of civil engineering continues to advance, the demands placed on construction materials like concrete have also grown exponentially.

*Corresponding author, Research Scholar, E-mail: gopalkpaliwal@gmail.com
[a] Ph.D.

 ISSN: 2234-0912 (Print), 2234-179X (Online)

To meet these evolving needs, concrete technology has undergone substantial development, enabling the production of innovative and specialized concrete types that outperform normal strength materials.

One such development is the introduction and widespread use of high strength concrete. This advanced material offers significant advantages over normal strength concrete by enabling the construction of structures that can carry larger loads while utilizing smaller cross-sectional dimensions. According to the guidelines outlined in IS: 10262-2019, concrete with compressive strength up to 60 MPa is classified as normal strength concrete, while concrete exceeding 60 MPa is considered high strength concrete. The adoption of high strength concrete has gained momentum globally due to its numerous benefits, including reduced member sizes, which result in lighter structures, enhanced durability that prolongs the lifespan of buildings and improved resistance to environmental degradation. Despite these advantages, the efficient use of high strength concrete in practical applications requires a thorough understanding of its material behavior, particularly its response to various loading conditions.

One of the most critical aspects of understanding concrete's behavior is analyzing its stress-strain relationship. This relationship describes how concrete deforms under stress, providing insights into its load-deformation characteristics. The stress-strain relationship is a foundational tool for the structural analysis and design of concrete elements, as it helps engineers predict how concrete will perform under real-world conditions. Understanding this relationship is particularly crucial for high-strength concrete, as its behavior differs significantly from that of normal strength concrete, especially in the post-peak region, where cracks and other failure mechanisms come into play.

Over the decades, numerous models have been proposed by researchers to describe the stress-strain behavior of concrete. These models aim to provide accurate mathematical representations of the relationship, enabling engineers to design safer and more efficient structures. This study examines several key models, starting with early foundational work and progressing to more recent developments. The models are presented using normalized parameters such as normalized stress ($\bar{\sigma}$), normalized strain ($\bar{\varepsilon}$), peak stress (σ_o) and peak strain (ε_o). Hognestad (1951) introduced a two-degree parabolic equation, $\bar{\sigma} = 2\bar{\varepsilon} - \bar{\varepsilon}^2$ to model the stress-strain variation in concrete. This equation predicts a zero stress in the post-peak region when strain reaches twice the peak strain, thus failing to account for residual stress after the peak. Later, Desayi and Krishnan (1964) proposed an alternative model, given as $\bar{\sigma} = \frac{2\bar{\varepsilon}}{1+\bar{\varepsilon}^2}$. Popovics (1973) and Carreira and Chu (1985) then enhanced this model by introducing a parameter, β, to improve its accuracy up to the ultimate point: $\bar{\sigma} = \frac{\beta\bar{\varepsilon}}{\beta-1+\bar{\varepsilon}^{\beta}}$. The equation $\beta = 1 + 0.058\sigma_o$ is used in Popovics (1973) model, while Carreira and Chu (1985) used $\beta = \frac{1}{1-\frac{\sigma_o}{\varepsilon_o E_{it}}}$. When β is 2, the model reverts to Desayi and Krishnan's form. However, even with β, the predictions for the descending branch found unsatisfactory still. To address this, Wee *et al*. (1996) modified Carreira and Chu (1985) equation as $\bar{\sigma} = \frac{k_1\beta\bar{\varepsilon}}{k_1\beta-1+\bar{\varepsilon}^{k_2\beta}}$, with $\beta = \frac{1}{1-\frac{\sigma_o}{\varepsilon_o E_{it}}}$. For concrete with compressive strength less than 50 MPa, $k_1 = k_2 = 1$ for both branches, but for compressive strength more than 50 MPa, $k_1 = k_2 = 1$ for the ascending branch and $k_1 = \left(\frac{50}{\sigma_o}\right)^3$ & $k_2 = \left(\frac{50}{\sigma_o}\right)^{1.3}$ for the descending branch. This modification aligned well with experimental data, though a tangent discontinuity at peak stress remained. Another model, proposed

by Sargin *et al*. (1971) for normal-strength concrete, is expressed as $\bar{\sigma} = \frac{A\bar{\varepsilon}+(D-1)\bar{\varepsilon}^2}{1+(A-2)\bar{\varepsilon}+D\bar{\varepsilon}^2}$, where $A = \frac{E_{it}}{(\frac{\sigma_o}{\varepsilon_0})}$ *and* $D = 0.65 - 7.25\,X\,10^{-3}\sigma_o$. To extend its applicability to a broader range of concrete grades, Wang *et al*. (1978) further modified this model, introducing the equation given as $\bar{\sigma} = \frac{A\bar{\varepsilon}+B\bar{\varepsilon}^2}{1+C\bar{\varepsilon}+D\bar{\varepsilon}^2}$, where A, B, C and D are distinct sets of coefficients for the ascending and descending branches of the stress-strain curve. Further, building on the Sargin *et al*. (1971) model, the CEB-FIP Model Code (1990) introduced a refined modification, extending its applicability to both normal and high strength concrete. The adopted equation given as $\bar{\sigma} = -\frac{\frac{E_{it}}{E_o}\bar{\varepsilon}-\bar{\varepsilon}^2}{1+(\frac{E_{it}}{E_o}-2)\bar{\varepsilon}}$, where $E_{it} = 9979.4\,\sigma_o^{\frac{1}{3}}$ *and* $E_o = \frac{\sigma_o}{\varepsilon_o}$. However, this model assumes a fixed peak strain of 0.002, conflicting with experimental evidence that shows peak strain increases with concrete strength. Also, Hsu and Hsu (1994) proposed a new model, claiming that it is simple and capable of predicting the complete stress-strain curve of high strength concrete with a compressive strength exceeding 69 MPa. The stress-strain relationship is given by the equation $\bar{\sigma} = \frac{n\beta\bar{\varepsilon}}{n\beta-1+\bar{\varepsilon}^{n\beta}}$, with $\beta = \left(\frac{\sigma_o}{65.23}\right)^3 + 2.59$ and the value of n depends on the compressive strength of the concrete: it is 1 for compressive strength below 62 MPa, 2 for strengths ranging from 62 to 76 MPa, 3 for strengths between 76 and 90 MPa, and 4 for compressive strength exceeding 90 MPa. Notably, this equation is derived by modifying the Carreira and Chu (1985) model. Finally, Wisam and Dina (2023) proposed a new model, $\bar{\sigma} = \bar{\varepsilon}^{\beta}$, where β differs for the ascending and descending branches. For the ascending branch, $\beta = \frac{0.7(\,1-\bar{\varepsilon}\,)\,\sigma_o^{\frac{1}{15}}}{1-(\,0.02\,\sigma_o^{0.8}\,)\bar{\varepsilon}}$ while for the descending branch, $\beta = \frac{\left(0.02\,\sigma_o^{\frac{4}{3}}\right)^{\bar{\varepsilon}}\,[1-\bar{\varepsilon}\,\left(0.02\,\sigma_o^{\frac{4}{3}}\right)]}{1+\bar{\varepsilon}\,\left(0.02\,\sigma_o^{\frac{4}{3}}\right)}$.

While these models generally align well with the experimental data used during their development, their applicability to diverse concrete grades. This study evaluates selected concrete models from the literature using a wide range of stress-strain data, encompassing ten stress-strain curves for concrete with peak compressive stresses from 18 MPa to 121 MPa. Models tailored to specific cases, say for example, high strength concrete, were excluded to focus on identifying universal models applicable to all concrete grades. Whereby five stress-strain models were chosen, starting with Hognestad (1951) and progressing through Sargin *et al*. (1971), Popovics (1973), Wee *et al*. (1996) and the most recent by Wisam and Dina (2023). A comparative analysis was conducted through graphical comparisons of measured versus predicted outcomes. Additionally, normalized toughness and ductility indices were calculated, and statistical tools such as the Coefficient of Variance and Root Mean Square were used to assess model performance.

2. Assessment of available models

The assessment of the selected stress-strain models was a thorough and multi-faceted process that employed graphical, analytical and statistical approaches. Each approach was carefully designed to evaluate the predictive accuracy of the models, ensuring their suitability for different grades of concrete, ranging from normal strength to high strength concrete. This comprehensive methodology

aimed to provide a holistic understanding of the strengths and limitations of the models, enabling informed conclusions about their applicability to real-world engineering problems.

The first step in evaluating the models was a graphical assessment, which involved comparing their predicted stress-strain curves with experimentally measured data. Experimental stress-strain curves were obtained from reputable studies by researchers such as Smith and Young (1956), Wang *et al*. (1978), Hsu and Hsu (1994), Wee *et al*. (1996) and Xiao *et al*. (2005). These studies provided a rich dataset encompassing a wide range of concrete peak stress, from as low as 18 MPa to as high as 121 MPa. This diverse range was selected to ensure that the assessment covered both normal strength concrete and high strength concrete, capturing the behavior of materials used in various structural applications.

However, a significant challenge in directly comparing stress-strain curves from different sources was the variation in peak stress and peak strain values across datasets. In absolute terms, the curves exhibited differing maximum points, making it difficult to overlay and compare them meaningfully. To address this issue, a normalization technique was employed. In this process, the stress values of each curve were divided by the respective peak stress, and the strain values were divided by the corresponding peak strain. This normalization produced dimensionless stress-strain curves, which facilitated consistent comparisons between datasets, regardless of their absolute values.

The normalized stress-strain curves were then plotted alongside the predictions from the selected models. Separate graphical analyses were performed for normal strength concrete (Fig. 1) and high strength concrete (Fig. 5), providing a visual representation of each model's ability to replicate the experimental data. This graphical approach allowed for an intuitive assessment of the performance of models, highlighting areas where the predictions aligned well with the measured curves and where deviations occurred. It also offered insights into how well each model captured key characteristics of the stress-strain relationship, such as the shape of the ascending and descending branches and the transition around the peak stress.

Building on the graphical analysis, an analytical evaluation was conducted to provide a quantitative measure of the performance of various selected models. This evaluation focused on the areas under the stress-strain curves, which represent the energy absorption capacity or toughness, of the material. The area under each curve was divided into two distinct regions: A_1, the area up to the peak stress, and A_2, the area beyond the peak stress. The sum of these two areas (A) represents the normalized toughness of the concrete, a critical parameter for assessing its ability to withstand loads without failure.

In addition to calculating toughness, the ductility of the material was assessed using the ductility index (μ), defined as the ratio of the post-peak area (A_2) to the total area (A). The ductility index provides valuable insights into the material's ability to sustain deformation beyond its peak load, a key consideration in structural applications where ductility is essential for safety and performance. Tables 1 and 2 summarize the calculated values of normalized toughness and ductility index for both normal strength and high strength concrete. By comparing these parameters across models, the analytical evaluation highlighted how well each model captured the energy-absorption and deformation characteristics of concrete under varying conditions.

The final component of the assessment involved a statistical analysis, which provided a more rigorous evaluation of the predictive accuracy. Two key statistical metrics were used: the Root Mean Square (RMS) and the coefficient of variance (V). The RMS value measures the standard deviation of the predicted stress values from the experimental data points. A lower RMS value indicates a better fit, suggesting that the model closely approximates the actual behavior of the material. Conversely, a higher RMS value implies greater deviations between the model and the experimental

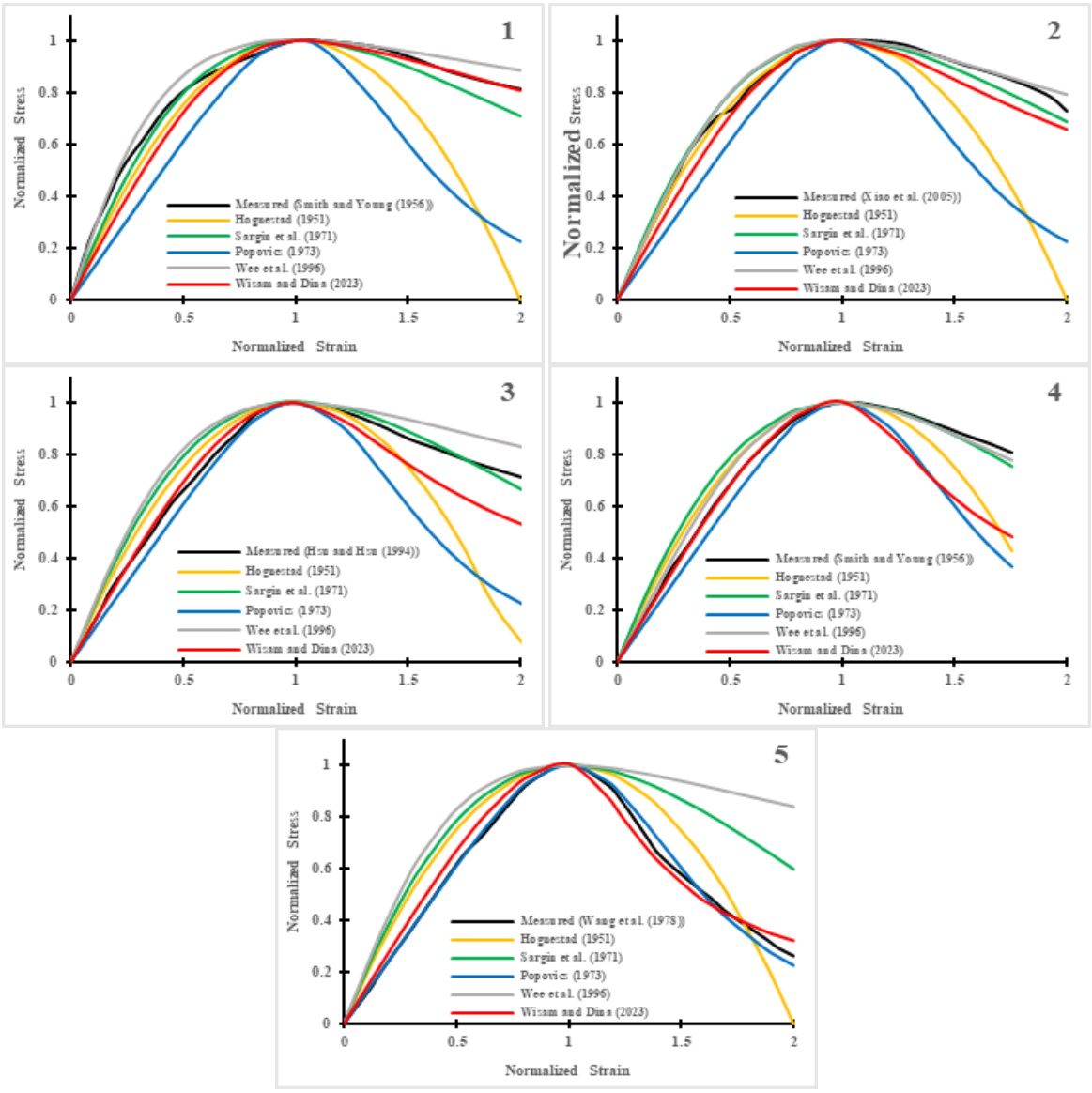

Fig. 1 Comparison of predictions from various models with the measured stress–strain relationships (in normalized form) for concrete with peak compressive stress as (1) 18 MPa, (2) 26 MPa, (3) 33 MPa, (4) 43 MPa, (5) 50 MPa

data, highlighting potential inaccuracies in the predictions. The coefficient of variance quantifies the scatter of data around the mean value. This metric is particularly useful for assessing the consistency of predictions of models. A lower variance indicates that the data points are tightly clustered around the mean, reflecting greater reliability in the performance of models. Conversely, a higher variance suggests greater dispersion in the data, which could indicate limitations in the ability of models to generalize across different datasets.

To evaluate these statistical parameters, corresponding to ‘n’ values of strain, the measured and

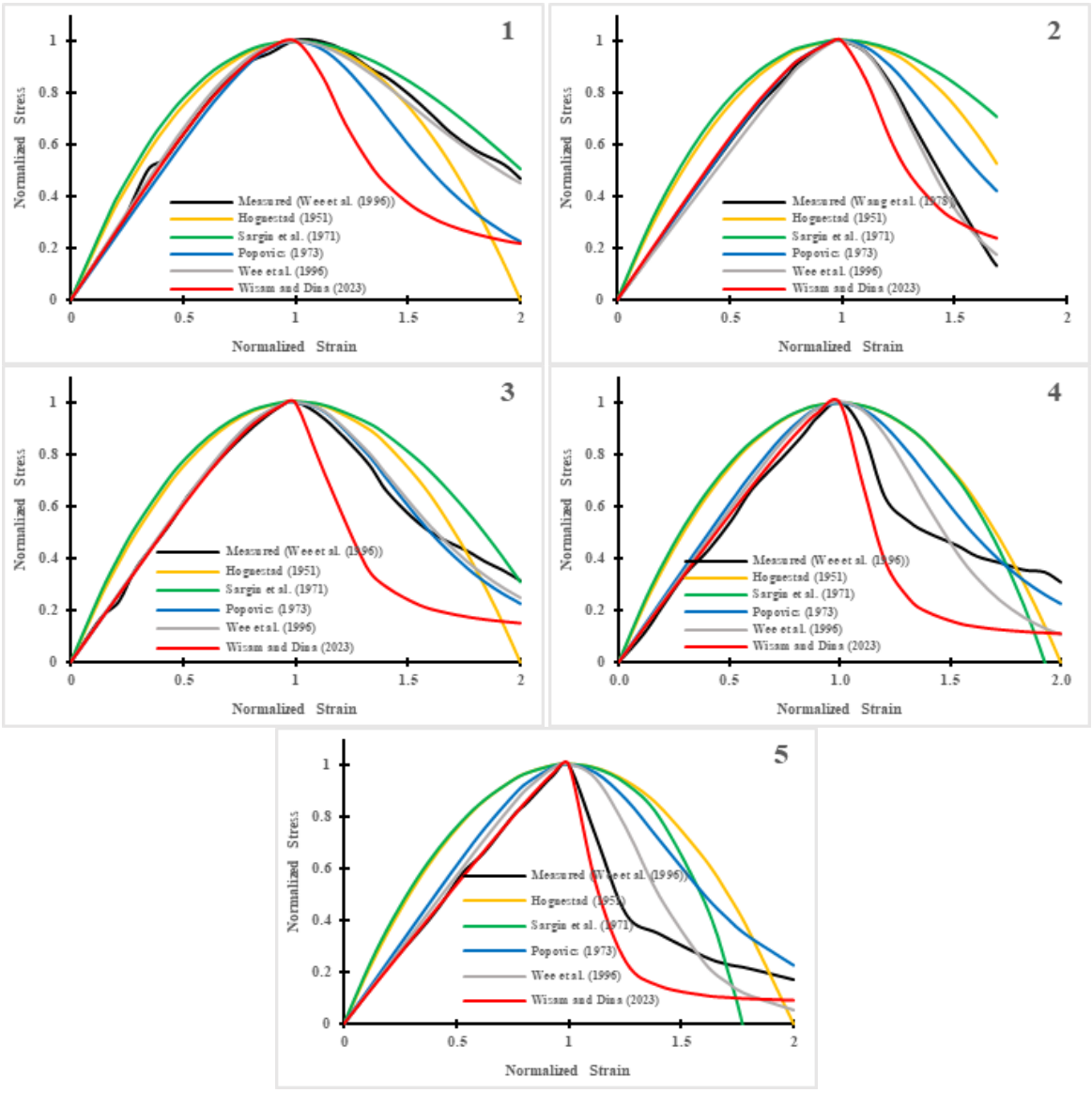

Fig. 2 Comparison of predictions from various models with the measured stress–strain relationships (in normalized form) for concrete with peak compressive stress as (1) 66 MPa, (2) 74 MPa, (3) 86 MPa, (4) 107 MPa, (5) 121 MPa

predicted (as per the model under consideration) stress values have been utilized as input into Eqs. (1) and (2) in the study. This systematic approach ensured that the evaluation covered the entire stress-strain curve, capturing variations in model performance across both the ascending and descending branches. The resulting RMS and variance values were summarized in Table 3, with separate columns for normal strength and high-strength concrete. These statistical metrics provided a robust measure of the accuracy and consistency of models, complementing the insights gained from the graphical and analytical evaluations.

Table 1 Estimated areas under measured and predicted normalized stress-strain curves for normal strength concrete

Peak compressive stress (MPa)	Parameter	Measured	Hognestad (1951)	Popovics (1973)	Sargin *et al*. (1971)	Wee *et al*. (1996)	Wisam and Dina (2023)
18	A_1	0.84	0.80	0.72	0.83	0.88	0.78
	A_2	0.78	0.52	0.48	0.74	0.81	0.78
	A	1.62	1.32	1.19	1.57	1.69	1.56
	μ	0.48	0.39	0.40	0.47	0.48	0.50
26	A_1	0.91	0.90	0.81	0.93	0.93	0.87
	A_2	0.77	0.73	0.41	0.72	0.78	0.69
	A	1.67	1.63	1.22	1.65	1.70	1.56
	μ	0.46	0.45	0.34	0.44	0.46	0.44
33	A_1	0.82	0.87	0.78	0.89	0.91	0.83
	A_2	0.66	0.62	0.42	0.66	0.72	0.57
	A	1.48	1.48	1.19	1.55	1.63	1.39
	μ	0.45	0.42	0.35	0.43	0.44	0.41
43	A_1	0.73	0.83	0.74	0.85	0.88	0.77
	A_2	0.58	0.44	0.38	0.52	0.46	0.41
	A	1.32	1.27	1.12	1.37	1.34	1.17
	μ	0.44	0.35	0.34	0.38	0.35	0.35
50	A_1	0.73	0.83	0.74	0.85	0.88	0.77
	A_2	0.45	0.50	0.45	0.68	0.77	0.44
	A	1.18	1.33	1.19	1.53	1.64	1.20
	μ	0.38	0.38	0.38	0.44	0.47	0.36

$$\mathrm{RMS} = \sqrt{\frac{\sum_{i=1}^{n}(m_i - p_i)^2}{n}} \tag{1}$$

$$V = 1 - \frac{\sum_{i=1}^{n}(m_i - p_i)^2}{\sum_{i=1}^{n} p_i^2} \tag{2}$$

Here,
m_i: Measured value of i^{th} stress,
p_i: Predicted value of i^{th} stress and
n: Total number of observations (stress-strain values) under consideration.

3. Results and discussion

By combining graphical, analytical and statistical methods, the assessment provided a comprehensive evaluation of the selected stress-strain models across normal to high strength concrete. The graphical analysis offered a visual understanding of the model predictive capabilities,

Table 2 Estimated areas under measured and predicted normalized stress-strain curves for high strength concrete

Peak compressive stress (MPa)	Parameter	Measured	Hognestad (1951)	Popovics (1973)	Sargin *et al*. (1971)	Wee *et al*. (1996)	Wisam and Dina (2023)
66	A_1	0.71	0.78	0.69	0.80	0.72	0.70
	A_2	0.66	0.55	0.50	0.70	0.64	0.36
	A	1.37	1.33	1.19	1.50	1.36	1.06
	μ	0.48	0.41	0.42	0.47	0.47	0.34
74	A_1	0.68	0.77	0.68	0.79	0.66	0.69
	A_2	0.32	0.47	0.41	0.51	0.31	0.26
	A	1.00	1.24	1.10	1.30	0.97	0.94
	μ	0.32	0.38	0.38	0.39	0.32	0.27
86	A_1	0.70	0.79	0.71	0.81	0.71	0.69
	A_2	0.50	0.53	0.49	0.63	0.50	0.25
	A	1.19	1.33	1.19	1.43	1.21	0.93
	μ	0.42	0.40	0.41	0.44	0.41	0.26
107	A_1	0.63	0.77	0.68	0.78	0.67	0.64
	A_2	0.42	0.56	0.51	0.73	0.41	0.19
	A	1.05	1.33	1.20	1.51	1.08	0.83
	μ	0.40	0.42	0.43	0.48	0.38	0.23
121	A_1	0.63	0.78	0.70	0.79	0.67	0.62
	A_2	0.28	0.54	0.50	0.28	0.33	0.15
	A	0.91	1.33	1.20	1.07	1.00	0.77
	μ	0.31	0.41	0.42	0.26	0.33	0.19

the analytical evaluation quantified their ability to capture toughness and ductility, and the statistical metrics measured their accuracy and consistency across different datasets. Together, these methods highlighted the strengths and limitations of each model, providing valuable insights into their applicability to various concrete grades.

The graphical analysis involved plotting normalized stress-strain curves from experimental data against model predictions. For concrete with peak stresses up to 50 MPa, models by Wee *et al*. (1996) and Wisam and Dina (2023) closely matched the experimental data. Notably, Wee *et al*. performed well in both ascending and descending branches, capturing post-peak behavior accurately. For high strength concrete, Wee *et al*. (1996) consistently aligned with experimental results, especially in the descending branch. However, models by Hognestad (1951) and Sargin *et al*. (1971) displayed limited accuracy in capturing post-peak behavior, with steeper declines than observed in the test data. Across all grades of concrete, Wee *et al*. (1996) emerged as the most graphically consistent model, especially in high strength applications.

Furthermore, the analytical approach focused on calculating the areas under the normalized stress-strain curves. The finding for normal strength concrete suggested that Wee *et al*. (1996) yielded high toughness values (e.g., 1.64 at 50 MPa) with ductility indices closely matching the experimental benchmark, achieving a value of μ=0.47 compared to the measured μ=0.48. Wisam

Table 3 Observed values for Root Mean Square (RMS) and Coefficient of Variance (V) of the predictions

Peak compressive stress (MPa)	Parameter	Hognestad (1951)	Popovics (1973)	Sargin *et al*. (1971)	Wee *et al*. (1996)	Wisam and Dina (2023)
18	RMS	0.28	0.29	0.05	0.04	0.07
	V	0.81	0.76	0.99	0.99	0.99
26	RMS	0.28	0.27	0.04	0.03	0.06
	V	0.82	0.79	0.99	0.99	0.99
33	RMS	0.23	0.22	0.07	0.10	0.08
	V	0.88	0.87	0.99	0.98	0.99
43	RMS	0.13	0.18	0.07	0.03	0.14
	V	0.96	0.91	0.99	0.99	0.95
50	RMS	0.13	0.02	0.22	0.31	0.04
	V	0.97	0.99	0.92	0.86	0.99
66	RMS	0.16	0.14	0.08	0.02	0.24
	V	0.95	0.95	0.99	0.99	0.83
74	RMS	0.21	0.13	0.28	0.03	0.09
	V	0.92	0.96	0.88	0.99	0.98
86	RMS	0.13	0.04	0.14	0.03	0.19
	V	0.96	0.99	0.97	0.99	0.88
107	RMS	0.20	0.11	0.23	0.11	0.18
	V	0.92	0.97	0.90	0.97	0.88
121	RMS	0.24	0.17	0.22	0.11	0.10
	V	0.89	0.93	0.90	0.97	0.97

and Dina (2023) also provided good alignment but with slight underestimation in post-peak toughness. For high strength concrete Wee *et al*. (1996) again showed higher toughness values and ductility indices closer to measured data across high strength concrete ranges. For example, at 121 MPa, it achieved a toughness A= 1.07, while Hognestad (1951) and Popovics (1973) underpredicted both A and μ, indicating limitations in adapting to higher strengths. Thus, the analytical assessment underscores Wee *et al*. (1996) as consistently delivering better toughness and ductility.

To further validate model performance, the RMS and coefficient of variance were calculated, assessing deviations between measured and predicted stress values. For stresses around 18–50 MPa, Wee *et al*. (1996) and Sargin *et al*. (1971) demonstrated low RMS values (e.g., 0.04 and 0.05), with near-ideal variance values (V = 0.99), highlighting a strong fit for normal strength strengths. In contrast, Wisam and Dina (2023) had slightly higher RMS values, indicating minor deviations in some data points. For high strength concrete, Wee *et al*. (1996) maintained low RMS values (e.g., 0.02 at 66 MPa) and high variance scores (V = 0.99), suggesting strong consistency. The model by Hognestad (1951) yielded higher RMS, especially at peak stresses above 100 MPa, reflecting difficulties in accurately capturing the high-strength stress-strain profile. RMS values were generally lowest for Wee *et al*. (1996), averaging 0.03–0.04 for all concrete types, while variance remained close to 0.99, indicating high predictive accuracy. Models like Hognestad (1951) and Popovics (1973) performed less accurately, especially at higher stresses, with RMS values sometimes

doubling those of the Wee *et al*. (1996) model.

The combine results from graphical, analytical and statistical assessments provide comprehensive insights. For concrete below 60 MPa, models by Wee *et al*. (1996) and Sargin *et al*. (1971) are reliable choices, with Wee *et al*. (1996) showing superior accuracy in both peak and post-peak behavior. Analytical toughness and ductility indices corroborate these findings, showing alignment with experimental benchmarks. For concrete above 60 MPa, Wee *et al*. (1996) remains the most consistent across all metrics. It balances graphical alignment, toughness, ductility and statistical accuracy, marking it as a highly adaptable model for high strength concrete. The study revealed that while some models performed well for specific types of concrete, others demonstrated more universal applicability. By identifying these distinctions, the assessment not only evaluated the selected models but also provided a foundation for future research aimed at developing more accurate and versatile stress-strain models for concrete. Such advancements are essential for improving the design and performance of concrete structures, ensuring their safety, efficiency and durability in a wide range of applications.

4. Conclusions

This study examined five widely recognized stress-strain models for concrete by analysing their effectiveness across various concrete grades through graphical, analytical and statistical evaluations. The models under review included Hognestad (1951), Popovics (1973), Wee *et al*. (1996), Wisam and Dina (2023). These models were evaluated against stress-strain data for concrete with varying peak compressive stress between 18 MPa to 121 MPa, which are published by various researchers such as Smith and Young (1956), Wang *et al*. (1978), Hsu and Hsu (1994), Wee *et al*. (1996) and Xiao *et al*. (2005). By comparing model predictions to reported stress-strain data, significant insights were obtained into the strengths and limitations of each model for concrete.

The model proposed by Wee *et al*. (1996) demonstrated superior graphical fit, accurate toughness and ductility measures and the lowest RMS values, averaging around 0.03–0.04 across all data sets. Additionally, it achieved a coefficient of variance close to 0.99, indicating minimal deviations and high consistency. In contrast, the Hognestad (1951) model has been widely adopted by various international design codes and researchers in concrete modeling due to its simplicity. It is well-suited for many applications, particularly for concrete with a lower range of compressive strength, while other models provide enhanced precision across a broader range, including high strength concrete scenarios. The model struggled to capture post-peak behavior, leading to higher RMS values (sometimes twice that of the Wee *et al*. model) and greater deviations from experimental results in both toughness and ductility. As a result, its applicability is more specialized rather than universal across all concrete types.

This study concludes that the modifications introduced by Wee *et al* (1996) to the Carreira and chu's model (1985) resulted in a model that showed strong agreement with reported experimental data. However, the model includes two sets of equations, one for concrete with a strength of less than 50 MPa and another for concrete with a strength greater than 50 MPa. As a result, multiple equations are necessary to deal for predicting stress-strain values, which complicates the process. This highlights the need for a novel model with single equation that incorporates easily measurable parameters, such as compressive strength, to ensure applicability to all grades of concrete. Thus, use of multiple equations can be avoided.

References

ACI 318-19 (2022), *Building Code Requirements for Structural Concrete*, American Concrete Institute, Farmington Hills, MI, U.S.A.

Carreira, D.J. and Chu, K.H. (1985), "Stress-strain relationship for plain concrete in compression", *ACI J.*, **82**(6), 797-804

CEB - FIP Model Code (1990), *Design Code - Comite Euro-International Du Beton*, Thomas Telford Ltd., London, U.K.

Desayi, P. and Krishnan, S. (1964), "Equation for the stress-strain curve of concrete", *ACI J.*, *Proceedings V*, **61**(3), 345-350.

Hognestad, E. (1951), "A study of combined bending and axial load in reinforced concrete members", *Bull. Ser.*, 399, Univ. Illinois Engineering Experimental Station, Champaign, IL, U.S.A.

Hsu, L.S. and Hsu, C.T.T. (1994), "Complete stress-strain behavior of high-strength concrete under compression", *Mag. Concr. Res.*, **46**(169), 301-312. https://doi.org/10.1680/macr.1994.46.169.301

Guo, Z.H. and Zhang, X.Q. (1982), "Experimental investigation of stress-strain curves for concrete", *Chinese J. Build. Struct.*, **3**(1), 1-12 (only available in Chinese language).

IS 456 (2000), *Plain and Reinforced Concrete - Code of Practice*, Bureau of Indian Standards, New Delhi, India.

IS 10262 (2019), *Concrete Mix Proportioning — Guidelines*, Bureau of Indian Standards, New Delhi, India.

Paliwal, G. and Maru, S. (2017), "Effect of fly ash & plastic waste on mechanical & durability properties of concrete", *Adv. Concr. Constr.*, **5**(6), 575. https://doi.org/10.12989/acc.2017.5.6.575

Popovics, S. (1973), "A numerical approach to the complete stress-strain curve of concrete", *Cem. Concr. Res.*, **3**(5), 583-599. https://doi.org/10.1016/0008-8846(73)90096-3

Sargin, M., Ghosh, S.K. and Handa, V.K. (1971), "Effects of lateral reinforcement upon the strength and deformation properties of concrete", *Mag. Concr. Res.*, **23**(75-76), 99-110.

Muralidhar, S.P. and Vesmawala, G.R. (2020), "Performance of concrete modified with SCBA and GGBFS subjected to elevated temperature", *Adv. Mater. Res.*, **9**(3), 203. https://doi.org/10.12989/amr.2020.9.3.203

Smith, G.M. and Young, L.E. (1956), "The complete stress-strain curve of concrete", *ACI J.*, *Proc.*, **53**, 597-609.

Tehmina, A., Nasir, S. and Fadhil, N. (2014), "Stress-strain response of high strength concrete and application of the existing models", *Res. J. Appl. Sci.*, **8**(10), 1174-1190. https://doi.org/10.19026/rjaset.8.1083

Van, G.A. and Taerwe, L. (1996), "Analytical formulation of the complete stress-strain curve for high strength concrete", *Mater. Struct.*, **29**, 529-533. https://doi.org/10.1007/BF02485952

Wang, P.T., Shah, S.P. and Naaman, A.E. (1978), "Stress-strain curves of normal and lightweight concrete in compression", *ACI J.*, **75**(11), 603-611. https://doi.org/10.14359/10973

Wee, T.H., Chin, M.S. and Mansur, M.A. (1996), "Stress-strain relationship of high-strength concrete in compression", *J. Mater. Civ. Eng.*, **8**(2), 70-76. https://doi.org/10.1061/(ASCE)0899-1561(1996)8:2(70)

Wen-Cheng, L., Wisena, P., En-Jui, L. (2015) "Compressive stress-strain relationship of high strength steel fiber reinforced concrete", *J. Adv. Concr. Technol.*, **13**, 379-392. https://doi.org/10.3151/jact.13.379

Wisam, H.S. and Dina, M.H. (2023), "Formulation of mathematical model for stress-strain relationship of normal and high strength concrete under compression", *Civil Environ. Eng.*, **19**(1), 119-133. https://doi.org/10.2478/cee-2023-0011

Xiao, J., Li, J. and Zhang, C. (2005), "Mechanical properties of recycled aggregate concrete under uniaxial loading", *Cement Concr. Res.*, **35**(6), 1187-1194. https://doi.org/10.1016/j.cemconres.2004.09.020

Zhao-Hui, L. and Yan-Gang, Z.M. (2010), "Empirical stress-strain model for unconfined high-strength concrete under uniaxial compression", *J. Mater. Civil Eng.*, **22**(11), 1181-1186. https://doi.org/10.1061/(ASCE)MT.1943-5533.0000095

Nomenclature

The following symbols are used in this paper:

β	Coefficient in stress-strain model proposed by researchers
σ	Stress (Absolute value of compressive stress)
ε	Strain (Absolute value corresponding to σ)
σ_o	Peak compressive stress (compressive strength)
ε_o	Peak strain (Strain value corresponding to σ_o)
$\bar{\sigma}$	Normalized stress ($\bar{\sigma} = \frac{\sigma}{\sigma_o}$)
$\bar{\varepsilon}$	Normalized strain ($\bar{\varepsilon} = \frac{\varepsilon}{\varepsilon_o}$)